BioNanoSci.
DOI 10.1007/s12668-016-0386-7

Tricalcium Phosphate Ceramics Doped with Silver, Copper, Zinc, and Iron (III) Ions in Concentrations of Less Than 0.5 wt.% for Bone Tissue Regeneration

I.V. Fadeeva[1] · M.R. Gafurov[2] · I.A. Kiiaeva[2] · S.B. Orlinskii[2] · L.M. Kuznetsova[3] · Ya.Yu. Filippov[4] · A.S. Fomin[1] · G.A. Davydova[5] · I.I. Selezneva[5] · S.M. Barinov[1]

© Springer Science+Business Media New York 2016

Abstract Novel materials with a variety of properties, such as biocompatibility, antibacterial activity, interconnected porosity, and functionalities combined in one, are required for regenerative medicine. Porous β-tricalcium phosphate (β-TCP) ceramics doped with Cu^{2+}, Zn^{2+}, Ag^{+}, and Fe^{3+} ions in the concentrations of less than 0.5 wt.% were synthesized and investigated. The obtained samples were analyzed by the diversity of analytical tools. The structure, solubility, and antimicrobial properties of the porous ceramics are shown to be very sensitive to the presence and the type of the cationic substituent. It opens the way to manage structure and properties of the materials for bone tissue regeneration by co-doping of the initial matrix simultaneously with different types of substituent ions.

Keywords Tricalcium phosphate · Regenerative medicine · Tissue engineering · Antibacterial properties

✉ I.V. Fadeeva
fadeeva_inna@mail.ru

[1] Institute of Metallurgy and Material Science RAS, Leninsky 49, Moscow, Russia 119334

[2] Kazan Federal University, Kremlevskaya 18, Kazan, Russia 420008

[3] Kazan State University of Architecture and Engineering, Zelenaya 1, Kazan, Russia 420043

[4] Research Institute of Mechanics Michurinsky 1, M.V. Lomonosov Moscow State University, Moscow, Russia 119192

[5] Institute of Theoretical and Experimental Biophysics of RAS, Institutskaya 3, Puschino, Moscow, Russia 142290

1 Introduction

Disease, injury, and trauma may lead to damage and tissues degradation in the human body. In the last decade, a novel concept for healing such injuries was provided, called bone tissue engineering (BTE) [1, 2]. The main idea of this concept is to regenerate damaged tissues, instead of replacing them. So, the matrix with complex properties is the key for successful implementation of such approach. A number of general considerations about the matrix are important for BTE approach: (1) biocompatibility, (2) biodegradability, (3) mechanical properties, and (4) architecture (that in the first instance means interconnected pore structure and high porosity to ensure cellular penetration and adequate diffusion of nutrients to cells within the construct and to the extracellular matrix formed by these cells) [3]. Calcium phosphates (CaP)-based ceramics are widely recognized as the most suitable matrix for bone tissue engineering [4–8]. The cationic and anionic substitutions of CaP structure by the elements and groups of biological importance seem to be the effective ways to improve the properties of CaP-based substances to achieve the material's desired parameters. A huge number of publications were and are devoted to the cationic substitutions in the hydroxyapatite (HA) structure. The main achievements in this field to date are reviewed in [5, 6].

Tricalcium phosphate in its β-form (β-TCP) is the other CaP which is considered as a potential material for matrixes in BTE approach. In spite of simple chemical formulae, β-TCP has a very complex structure and plenty of sites for the ionic incorporation even comparing to the hydroxyapatite [9–12]. But substituted β-TCP is studied much less than HA. The first results of a computational study of cationic incorporation in TCP were presented just recently [13]. Several works are devoted to Mg- and Zn-containing β-TCP [14, 15], but

Published online: 22 December 2016

interconnection between the doping, structure, and biological response (in particular, cytotoxicity) is still not clear.

Postoperative infection is known to be the most common complication in surgery also for the regenerative intervention. Antibiotics are usually used to prevent the revision operations. One of the ways to limit or even to avoid the prolonged course of antibiotics is the incorporation of antibacterial ions into the CaP structure [16]. That is an additional point of interest to the doped CaP.

Our work was aimed at the investigation of the cationic substitutions in the structure of β-TCP. We used traditional methods and electron paramagnetic resonance (EPR) for structure investigations and to establish the relationship between the structural changes and antibacterial activity of the materials developed.

2 Materials and Methods

β-TCP powders with Cu^{2+}, Zn^{2+}, Ag^{+}, or Fe^{3+} were synthesized by precipitation method from the nitrates aqueous solutions [17, 18]. For the divalent cations, the product reaction scheme can be represented as follows:

$$2.99CaO + 0.01M(NO_3)_2 + 2(NH_4)_2HPO_4 \rightarrow Ca_{2.99}M_{0.01}(PO_4)_2, \quad (1)$$

where M = Cu^{2+} and Zn^{2+}. Mono- and trivalent cations Ag^{+} and Fe^{3+} were incorporated in the same manner [19]. The obtained powders were treated at 900 °C during 1 h for TCP crystallization. The ceramic cylindrical discs of 6 mm in diameter and 2 mm in height obtained from the ceramic powders by pressing were sintered at 1100 °C during 2 h. The porous ceramic species were produced using negative replicas method by impregnating a cellular polymer scaffold matrix with slurry of polyacrylamide with ceramic powder followed by sintering at 1100 °C. The porous polyurethane matrix with a porosity of 15 pores per square centimeter was used as a template.

The species were studied by scanning electron microscopy (Tescan VEGA II), X-ray diffraction (Shimadzu 6000), IR spectroscopy (Nikolet Avatar 330 FT-IR), and electron paramagnetic resonance (Bruker Elexsys 580/680 and Bruker ESP-300) in the temperature range (15–300 K). Concentration of paramagnetic centers (PC) was estimated at room temperature in the double cavity ER4105DR by comparing the integrated intensities of the spectra of a test sample and a reference one (Mn^{2+} in MgO and organic radical DPPH) with the known concentrations of PC. Details of the quantitative analysis of EPR spectra one can found in ref. [20]. Integration was done in Origin 8.0 program.

Atomic emission spectroscopy with inductively coupled plasma (ICP-AES, Ultima-2) was applied to establish ions concentrations in the solubility experiment. The solubility was investigated in the isotonic (0.9% sodium chloride) solution with pH = 7.4 at 37 °C. The porosity was measured with a Micromeritics Tristar 3000 using nitrogen as the working gas.

NCTC murine fibroblasts (clone L929, ATCC CCL1) were used to study the biocompatibility of the TCP ceramics and TCP ceramics doped with Ag^{+}, Fe^{3+}, Zn^{2+}, and Cu^{2+}. The culture medium DMEM/F12 containing 100 units per milliliter of penicillin/streptomycin was selected as model medium. The fibroblasts of NCTC L929 line were used for the experiments.

The method of direct contact was applied to study the adhesive characteristics of materials and for the determination of their cytotoxicity to the cells. Separation of cell types in mixed culture was carried out using the difference in the adhesion of various cell types to the surface of the cultivation.

The cytotoxicity was evaluated through cell culture (elution assay and MTT test). The antimicrobial activity was examined for *Escherichia coli* strains using Muller–Hinton agar according to [21] (see also [22] for a review). Statistical processing of the results was performed using Origin program, and standard deviation for the mean value was taken (Mann–Whitney U test, $p < 0.05$).

3 Results and Discussion

According to elemental analysis, Cu^{2+}, Zn^{2+}, Ag^{+}, and Fe^{3+} ions are found in TCP samples in the amounts that were used during the synthesis (Table 1) and correspond to those calculated for the formula $Ca_{2.99}M_{0.01}(PO_4)_2$

XRD analysis shows that all the TCPs-substituted compounds possess whitlockite structure (JCPDS card no. 09-0169). No one other crystal phases was found. It is known [23] that cationic substitutions significantly affect the temperature T_{trans} for α-β transition of TCP structure: T_{trans} may change from 1300 up to 1200 °C. Our samples were calcined at 900 °C, that is why we did not observe any perceptible differences in XRD spectra.

Modes at 1030, 970, and (560–610) cm^{-1} in IR spectra were attributed to PO_4, and wide band in the region (2700–3600) cm^{-1} was attributed to the adsorbed water molecules. Earlier, it was reported that Mg substitution could lead to the perceptible widening of PO_4 bands [14]. No observable differences were found between the IR spectra for cation substituted and non-substituted β-TCP in our experiments that could be explained by the low concentrations of the impurity ions.

EPR spectrum of CuTCP taken at room temperature differs significantly from the non-doped TCP (Fig. 1). The signals of incorporated manganese Mn^{2+} ions in concentration of

Table 1 The antimicrobial activity and cytotoxic properties of TCP-substituted compounds

ID	Dopant ion	wt.% of dopant from elemental analysis data	wt.% of dopant calculated for $Ca_{2.99}M_{0.01}(PO_4)_2$	Diameter inhibition halo in mm according to NCCLS	Cell viability, percentage of control
AgTCP	Ag	0.335	0.341	24 ± 1	107 ± 14
FeTCP	Fe	0.168	0.179	26 ± 5	112 ± 10
CuTCP	Cu	0.20	0.205	27 ± 7	102 ± 9
ZnTCP	Zn	0.20	0.208	34 ± 1	87 ± 8
TCP	Non-doped	–	–	0	102 ± 5

$0.3{\cdot}10^{19}$ spins per gram (g^{-1}) are registered [24, 25]. In non-substituted TCP, the EPR is probably due to contamination of the starting materials (calcium nitrate and ammonium dihydrophosphate) with manganese.

Although the position and lineshape of EPR spectrum for CuTCP at room temperature is undoubtedly due to the Cu^{2+} ions [26, 27], EPR measurements were performed at $T = 15$ K (Fig. 2) to define the nature and EPR parameters of the paramagnetic species precisely. The EPR spectrum can be simulated nicely with the anisotropic spin Hamiltonian (electron spin $S = ½$) taken into account the hyperfine interaction with the nuclear spin $I = 3/2$. Parameters of the simulation (see Fig. 2) coincide with the data of Mayer et al. [27] for "isolated" Cu^{2+} ions embedded into the TCP crystal structure. Quantitative analysis allows to estimate the concentrations of Cu^{2+} ions as $2.0{\cdot}10^{19}$ g^{-1}. It implies that more than 90% of copper in the investigated Cu-containing samples is in the Cu^{2+} state. This conclusion confirms the suggestion about the substitution of calcium ions with copper ions.

The total (effective) porosity increases in the row Ag<Fe<Cu<Zn from 65 to 85%, while the dominant pore diameter changes from 25(5) μm for Ag up to 150(50) μm for other dopants.

Figure 3 presents the data for the ion release from the set of samples ($n = 3$) by aging in solution during 30 days. The results appeared to be very puzzling for us. It is known that the solubility depends on many factors including the stoichiometry, porosity, local defects of the crystal lattice, ionic radius of the dopant, and its concentration (see [28] for the recent review). We are planning to repeat the solubility experiments for them for other concentrations of ions.

The antimicrobial activity was determined using the diffusion method. All the cation-substituted samples (especially with Zn^{2+}) reveal the obvious antimicrobial activity (Table 1). The antimicrobial activity of TCP-substituted compounds increases in series Ag<Fe<Cu<Zn. While for the HA-based materials, a sufficient amount of experimental data related to the influence of type of cationic dopant and its concentration onto the antimicrobial properties are gathered (see [29] for the recent review), not so much records for TCP exist.

Solid growth zone and the diameter of inhibition zone less than 10 mm showed no antimicrobial activity of the test sample to a given strain of microorganism; 10–15 mm diameter zones demonstrate weak activity; 15–20 mm—moderate; more than 20 mm—expressed.

The MTT assay data showed that new porous TCP ceramics and TCP ceramics doped with Ag^{+}, Fe^{3+}, and Cu^{2+}

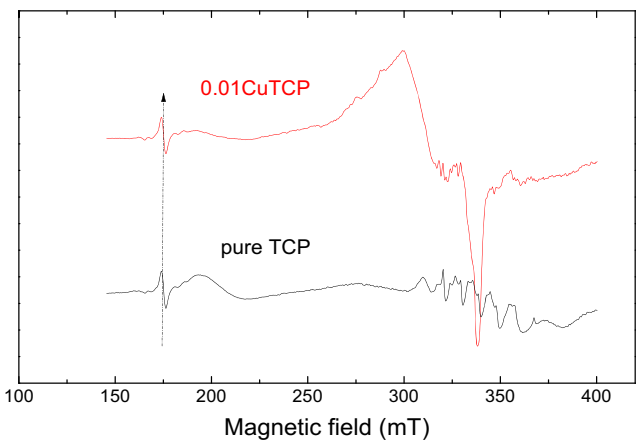

Fig. 1 EPR spectra of Cu-containing TCP (*upper*, *red curve*) and "pure" TCP (*lower*, *black curve*) taken at room temperature ($T = 300$ K). The *arrow* marks the signal caused by the cavity contamination

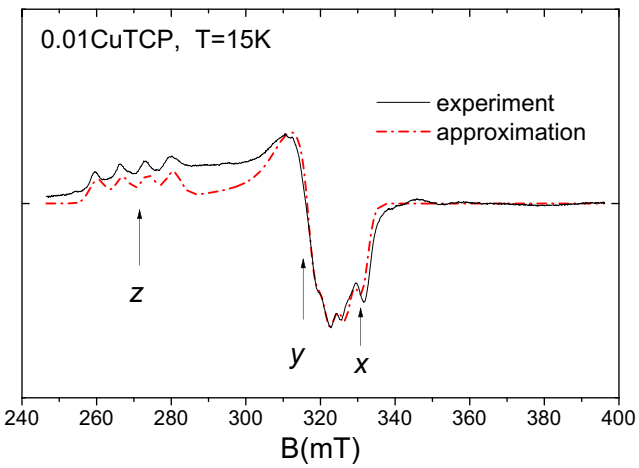

Fig. 2 A part of the EPR spectrum of Cu-containing TCP due to the Cu^{2+} ions detected at $T = 15$ K (*solid*, *red curve*) and its simulation (*red*, *dashed line*) with the parameters of the g-factor components of electron spin $S = ½$ $g_x = 2.076$; $g_y = 2.118$; $g_z = 2.493$ and the constants of the hyperfine interaction with the nuclear spin of $I = 3/2$ $A_x = 122$ MHz; $A_y = 122$ MHz; $A_z = 240$ MHz

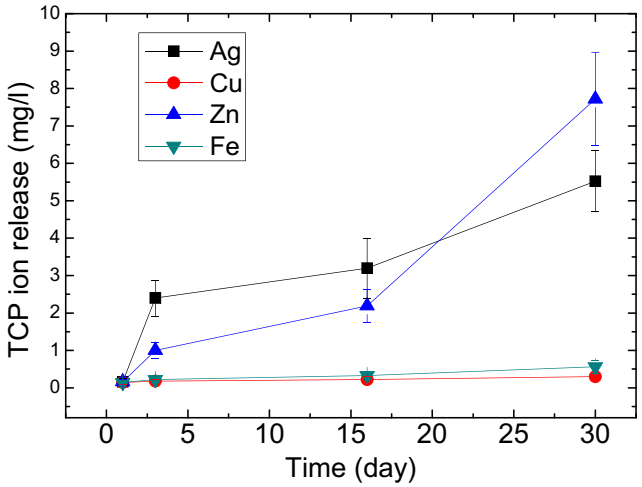

Fig. 3 Ion release from the set of Cu^{2+}, Zn^{2+}, Ag^{+}, or Fe^{3+}-containing TCP samples ($n = 3$) by aging in solution during 30 days (corresponding symbols) at physiological conditions. The *lines* are drawn to connect the experimental data

ions are biocompatible. The significant difference is observed in the cell viability between the TCP ceramics doped with Zn^{2+} ions and the control. Inhibition halo diameter of the TCP ceramics doped with Zn^{2+} ions was above 30 mm, while the inhibition of cell activity according to the MTT test occurred less than 15%. Consequently, to obtain cytocompatible materials having a pronounced antibacterial activity, concentration of Zn^{2+} ions should be (in our opinion) further decreased. This conclusion is partially based on the data provided in the review [29] for Zn-substituted HA.

The synthesis of TCP with different concentrations of the mentioned cations and their characterization are on the way.

4 Conclusions

New porous TCP ceramics doped with Ag^{+}, Fe^{3+}, Cu^{2+}, and Zn^{2+} ions were developed. The substituted ceramics were shown to have better solubility comparing with the non-doped TCP ceramics and to possess the antibacterial properties. The porous structure in combination with solubility in body's fluids as well as antibacterial properties makes the obtained ceramics perspective for the regenerative medicine.

Evidently, the knowledges of the material structure and properties depending on the synthesis way and followed treatment are necessary for a successful development of new multifunctional materials for regenerative medicine. It, in turn, implies the integrated theoretical and experimental approach to optimize the material production method. The way presented in this paper allows to create the materials for bone tissue regeneration by the co-doping of the initial TCP template simultaneously with different ions for the required properties of the matrix. Obviously, our next experimental and theoretical efforts will be aimed to define cation locations and the charge compensation schemes by using among others developed by us for the HA-substituted (nano)powders approach [9–12, 30].

Acknowledgements This work was financially supported by RFBR grant no. 15-08-06860-a, by the program of competitive growth of Kazan Federal University and the subsidy allocated to Kazan Federal University for the state assignment in the sphere of scientific activities.

Compliance with Ethical Standards

Conflict of Interest The authors declare that they have no conflict of interest.

Dedication MRG and SBO dedicate this work to Dr. I.N. Kurkin (Kazan) on occasion of his 75th birthday.

References

1. Burg, K. J. L., Porter, S., & Kellam, J. F. (2000). Biomaterial developments for bone tissue engineering. *Biomaterials, 21*, 2347–2359.
2. Komaki, H., Tanaka, T., Chazono, M., & Kikuchi, T. (2006). Repair of segmental bone defects in rabbit tibiae using a complex of β-tricalcium phosphate, type I collagen, and fibroblast growth factor-2. *Biomaterials, 27*, 5118–5126.
3. O'Brien, F. J. (2011). Biomaterials & scaffolds for tissue engineering. *Materials today, 14*, 88–95.
4. Barinov, S. M. (2010). Calcium phosphate-based ceramic and composite materials for medicine. *Russ Chem Rev, 79*, 13–29.
5. Uskovic, V., & Vu, V. M. (2016). Calcium phosphate as a key material for socially responsible tissue engineering. *Materials, 9*, 434(27).
6. Cacciotti, I. (2015). Cationic and anionic substitutions in hydroxyapatite. In I. V. Antoniac (Ed.), *Handbook of bioceramics and biocomposites* (p. 1068). Cham: Springer.
7. Barinov, S. M., & Komlev, V. S. (2008). *Calcium phosphate based bioceramics for bone tissue enginery*. Zurich: Trans Tech. Publ.
8. Hughes, J. M., & Rakovan, J. (2002). The crystal structure of apatite, $Ca_5(PO_4)_3(F,OH,Cl)$. *Rev Mineral Geochem, 48*, 1–12.
9. Gafurov, M., Biktagirov, T., Mamin, G., & Orlinskii, S. (2014). A DFT, X- and W-band EPR and ENDOR study of nitrogen-centered species in (Nano)hydroxyapatite. *Appl Magn Reson, 45*, 1189–1203.
10. Biktagirov, T., Gafurov, M., Mamin, G., et al. (2014). Combination of EPR measurements and DFT calculations to study nitrate impurities in the carbonated nanohydroxyapatite. *J Phys Chem A, 118*, 1519–1526.
11. Gafurov, M., Biktagirov, T., Mamin, G., et al. (2015). The interplay of manganese and nitrate in hydroxyapatite nanoparticles as revealed by pulsed EPR and DFT. *Phys Chem Chem Phys, 17*, 20331–20337.
12. Gafurov, M., Biktagirov, T., Mamin, G., et al. (2016). Study of the effects of hydroxyapatite nanocrystal codoping by pulsed electron paramagnetic resonance methods. *Phys Solid State, 58*, 469–474.
13. Matsunaga, K., Kubota, T., Toyoura, K., & Nakamura, A. (2015). First-principles calculations of divalent substitution of Ca^{2+} in tricalcium phosphates. *Acta Biomater, 23*, 329–337.
14. Bandyopadhyay, A., Bernard, S., Xue, W., & Bose, S. (2006). Calcium phosphate-based resorbable ceramics: influence of MgO, ZnO, and SiO_2 dopants. *J Am Ceram Soc, 89*(9), 2675–2688.
15. Fielding, G. A., Bandyopadhyay, A., & Bose, S. (2012). Effects of silica and zinc oxide doping on mechanical and biological properties of 3D printed tricalcium phosphate tissue engineering scaffolds. *Dent Mater, 28*, 113–122.

16. Raphel, J., Holodniy, M., Goodman, S. B., & Heilshorn, S. C. (2016). Multifunctional coatings to simultaneously promote osteointegration and prevent infection of orthopaedic implants. *Biomaterials, 84*, 301–314.
17. Barinov SM, Fadeeva IV, Fomin AS, Petrakova NV. (2015) Method of obtaining porous ceramics of calcium phosphates for the treatment of bone defects. RF Patent application № 2015–112518, date of priority 07.04.2015.
18. Fadeeva, I. V., Gafurov, M. R., Filippov, Y. Y., et al. (2016). Copper-substituted tricalcium phosphates. *Dokl Chem, 471*, 384–387.
19. Fadeeva, I. V., Selezneva, I. I., Davydova, G. A., et al. (2016). Iron-substituted tricalcium phosphate ceramics. *Dokl Chem, 468*, 159–161.
20. Eaton, G. R., Eaton, S. S., Barr, D. P., & Weber, R. T. (2010). *Quantitative EPR* (p. 185). New York: Springer, XII.
21. Semina, N. A., Sidorenko, S. V., Rezvan, S. P., et al. (2004). Guidelines for susceptibility testing of microorganisms to antibacterial agents: methodical instructions MUK 4.2.1890-04. *CMAC, 6*, 306–357 [in Russian].
22. Balouiri, M., Sadiki, M., & Ibnsouda, S. K. (2016). Methods for *in vitro* evaluating antimicrobial activity: a review. *J Pharm Anal, 6*, 71–79.
23. Choi, D., & Kumta, P. N. (2007). Mechano-chemical synthesis and characterization of nanostructured β-TCP powder. *Mater Sci Eng C, 27*, 377–381.
24. Galukhin, A., Khelkhal, M. A., & Gerasimov, A. V. (2016). Mn-catalyzed oxidation of heavy oil in porous media: kinetics and some aspects of mechanism. *Energy Fuel, 30*(9), 7731–7737.
25. Gafurov, M., Chelyshev, Y., Ignatyev, I., et al. (2016). Connection between the carotid plaque instability and paramagnetic properties of the intrinsic Mn^{2+} ions. *BioNanoSci, 6*, 558–560.
26. Burlaka, A. P., Gafurov, M. R., Iskhakova, K. B., et al. (2016). Electron paramagnetic resonance in the experimental oncology: implementation examples of the conventional approaches. *BioNanoSci., 6*, 431–436.
27. Mayer, I., Gdalya, S., Burghaus, O., & Reinen, D. (2009). A spectroscopic and structural study of $M(3d)^{2+}$-doped β-tricalcium phosphate—the binding properties of Ni^{2+} and Cu^{2+} in the pseudo-octahedral $Ca(5)O_6$ host-sites. *Z Anorg Allg Chem, 635*(12), 2039–2045.
28. Schumacher, M., & Gelinsky, M. (2015). Strontium modified calcium phosphate cements—approaches towards targeted stimulation of bone turnover. *J Mater Chem B, 3*, 4626–4640.
29. Kolmas, J., Groszyk, E., & Kwiatkowska-Różycka, D. (2014). Substituted hydroxyapatites with antibacterial properties. *Biomed Res Int, 2014*, 178123.
30. Yavkin, B. V., Mamin, G. V., Orlinskii, S. B., et al. (2012). Pb^{3+} radiation defects in $Ca_9Pb(PO_4)_6(OH)_2$ hydroxyapatite nanoparticles studied by high-field (W-band) EPR and ENDOR. *Phys Chem Chem Phys, 14*(7), 2246–2249.